GENERAL PHYSICS

I. MOLECULAR BEAMS*

Academic and Research Staff

Prof. J. R. Zacharias	Dr. D. S. Hyman	Dr. J. C. Weaver
Prof. J. G. King	Dr. E. H. Jacobsen	F. J. O'Brien
Prof. J. R. Clow	Dr. R. C. Pandorf	D. S. Ofsevit

Graduate Students

T. R. Brown	W. B. Davis	D. E. Oates
S. A. Cohen	G. A. Herzlinger	R. F. Tinker
	J. W. McWane	

A. SCATTERING OF LOW-TEMPERATURE HELIUM BEAMS

Recently, we have made measurements of the helium^4-helium^4 scattering cross section at very low temperatures by an atomic-beam method. The apparatus uses conventional atomic beam methods to determine the cross section; that is, a collimated beam of helium atoms is passed through a region of relatively high-pressure helium gas and attenuation of the beam is measured. The beam is detected by a field-ionization detector with an electron multiplier to count the positive ions produced. The apparatus differs, however, from the usual design, in that it is entirely immersed in a liquid-helium bath, whose temperature can be controlled by lowering the vapor pressure, and, also, the pumping to maintain the necessary high vacuum is done by cold zeolite pellets, which effectively adsorb helium when cooled to liquid-helium temperatures. The beam is chopped by a rotating slotted disk. The beam source and the scattering region are maintained at the temperature of the liquid-helium bath. Figure I-1 is a schematic view of the apparatus.

The electronics associated with the detection system is shown in Fig. I-2. The output pulses from the electron multiplier are amplified and fed into a 64-channel scaler whose channel advance circuit is initiated by the output pulses of a photomultiplier each time the beam chopper opens. This method measures the time of flight of the atoms in the beam. The beam atoms have an arrival time distribution because of their velocity distribution and the finite length of drift space between the chopper and detector. To obtain the total beam intensity, one simply integrates the area under the arrival-time distribution and above the uniform counts caused by the background pressure in the apparatus.

The effective total scattering cross section is determined by the standard formula:

*This work was supported by the Joint Services Electronics Programs (U.S. Army, U.S. Navy, and U.S. Air Force) under Contract DA 28-043-AMC-02536(E), and in part by the Sloan Fund for Basic Research (M.I.T. Grant 367).

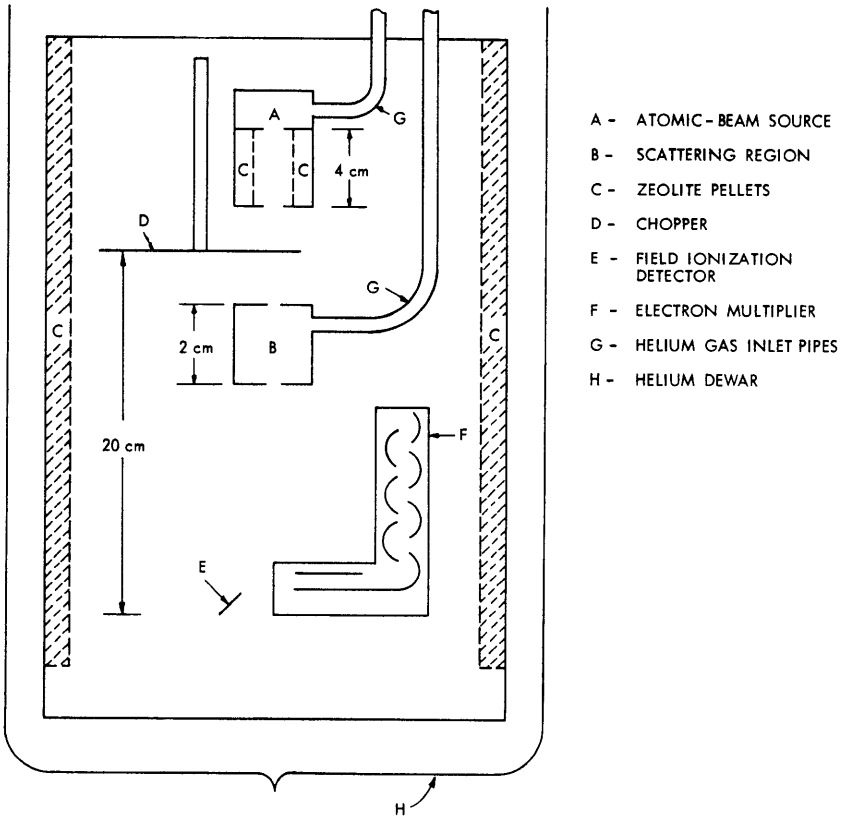

Fig. I-1. Schematic view of the apparatus.

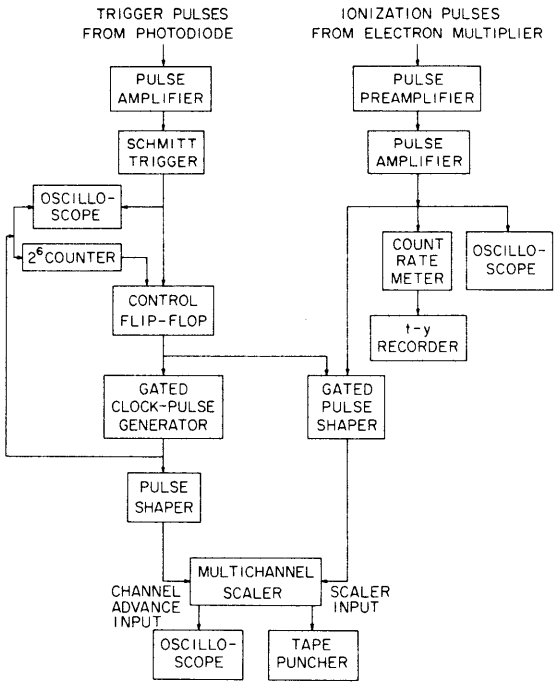

Fig. I-2. Electronic equipment for the detection system.

$$I = I_o e^{-x/\lambda},$$

where

I is the detected beam intensity in atoms/s.

I_o is the beam intensity with no scattering taking place.

x is the length of the region where scattering takes place.

λ is the mean-free path in the scattering region.

The effective scattering cross section σ is then given by

$$\lambda = \frac{.749}{n\sigma},$$

where n is the density of the atoms in the scattering region. This is under the assumption that the mean-free path everywhere except in the scattering region is large compared with λ, which is true in this case.

Experimentally, what one does is measure the beam intensity with the scattering chamber empty, that is, at high vacuum, thereby obtaining I_o, and then measure the beam intensity with a known pressure of helium gas in the scattering region and apply the formula above. The pressure in the scattering region is determined from measured flow rates of gas into it, which in the steady state must also be leaving through the slits of known area at the ends. Thus application of the formula from kinetic theory for molecular flow through an orifice gives the pressure and therefore the density in the scattering region. The formula is

$$I = \frac{3.5 \times 10^{22}\ PA}{\sqrt{MT}},$$

where

I is the number of atoms/s exiting.

P is the pressure inside in mm Hg.

A is the slit area in cm^2.

M is the mass of the atoms in atomic mass units.

T is the absolute temperature.

Experimental runs have been made at 2.1°K with pressures in the scattering region ranging from 3×10^{-6} to 1×10^{-5} mm Hg. These give, for the total effective cross section σ, a value of 79×10^{-16} cm^2 with an estimated error of 10%.

The cross section is a function of the velocity of the colliding atoms, however. The method described above averages this velocity-dependent cross section over the velocities in the beam and over the velocities in the scattering gas. By measuring the arrival-time distribution of the beam as we do, we have information on the velocity distribution in the beam both with scattering and without. This information can then

be used to obtain the effective cross section as a function of beam velocity, which contains only an average of the actual cross section over the velocity distribution in the scattering gas. At the present time, the signal noise of the data is not sufficient to allow us to do this, We are in the process of getting more data in hopes of increasing the signal-to-noise ratio sufficiently, so that the cross section as a function of beam velocity can be determined over a reasonable range of velocities.

We also intend to measure the cross sections for helium^3 on helium^4 and helium^3 on helium^3, which can be done with no modifications to the present apparatus.

D. E. Oates

B. FIELD DISTRIBUTION MEASUREMENTS BY THE ATOMIC-BEAM METHOD

There are many methods for measuring magnetic microstructure in solids, and they have been widely used to contribute largely to the understanding that we now have of magnetic materials. In this report we describe a new way of investigating magnetic systems, using the classical atomic-beam magnetic-resonance method.

In this method transitions between the states of an atom in a magnetic field are produced by applied radio-frequency fields and detected by observing the subsequent trajectory of the atom through the apparatus (Fig. I-3). The magnetic properties of many atoms have been studied by this method, so that with confidence we can use the atoms to study magnetic fields with variations in space and time on scales that made them hard to measure by other means.

So-called Type II superconductors exhibit magnetic structure on a scale of the order of 1,000-10,000 A when the applied magnetic fields penetrate and produce quantized vortices of electrons (Fig. I-4). Recently, an application of the Bitter powder technique has allowed a direct picture of the vortices to be built up from small (100 A) iron particles (Fig. I-5a; see Trauble and Essmann[1]). These patterns are later observed with an electron microscope and have yielded much information concerning the arrangement of magnetic fields in samples. Unfortunately, the method does not lend itself to the study of rapid variations; thus, when a current is applied merely a smear is seen as the vortices are transported by the current at right angles to both the current and the magnetic field. No convincing measurement of the velocity of the vortices has been made until now. Since the motion of these vortices accounts for various technical limitations on the use of the superconductors in wide-scale practical engineering applications, understanding their motion and the associated pinning forces is of considerable importance.

If we arrange an apparatus so that the atoms of the beam pass near the surface of a Type II superconductor, they will be passing through a spatially varying magnetic

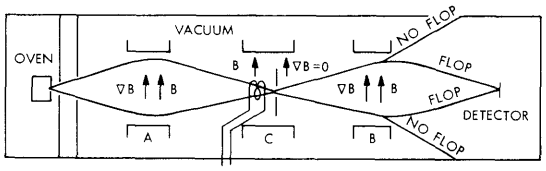

Fig. I-3. Detection techniques.

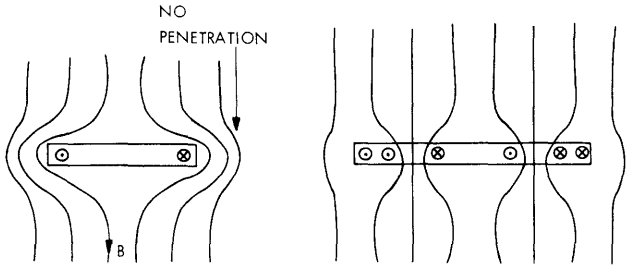

Fig. I-4. Production of quantized vortices of electrons.

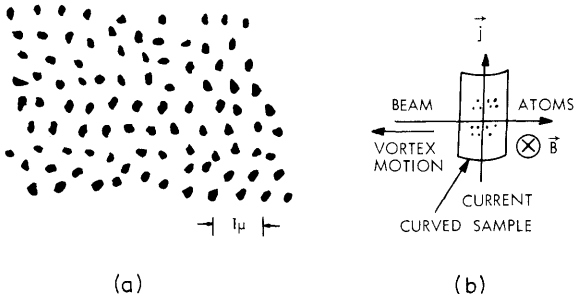

Fig. I-5. Illustrating the Bitter powder technique.

field. They will, therefore, experience a periodic field in time whose frequency is proportional to the spacing of the vortices. If this frequency coincides with the transition frequency between two states of the atom, transitions will occur and can be detected in the usual way. By chopping the beam and analyzing the arrival-time distribution of the atoms that have undergone transitions, we can deduce their velocity and hence the spacing of the magnetic field periodicity. When current is applied to the sample at right angles to the magnetic field and to the beam direction (Fig. I-5b), the vortices move and a Doppler shift is observed.

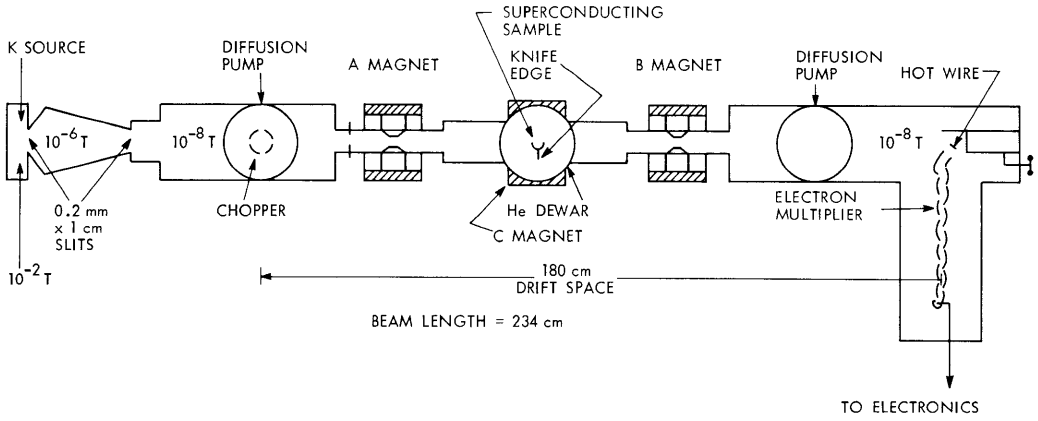

Fig. I-6. The apparatus.

Figure I-6 is a drawing of the apparatus which will be recognized as a conventional atomic-beam apparatus equipped with a chopper and time-of-flight analysis of the velocity of the flopped atoms. Instead of the usual magnet and sources of oscillating magnetic fields, it contains a vanadium foil past which the beam travels. The foil can be cooled below its transition temperature and subjected to magnetic fields and currents. A typical result of a 1-min run is shown in Fig. I-7 in which the relative transition probability normalized as a fraction of the maximum obtainable flop from RF is plotted as a function of the velocity of the atom. The markedly non-sinusoidal oscillations are what would be expected from the space frequencies of a two-dimensional triangular lattice forming an angle with respect to the beam. In Fig. I-8 we show the same curve and two others in which a current has been applied to the sample, first in one direction and then the other. These curves are recognizable as the curve obtained when no current flows shifted in velocity, since the atoms are now going by moving vortices. Some of the features are washed out by this current and the resultant motion of the vortex lattice, as might well be expected. Data from a number of runs can be summarized by the curve of Fig. I-9, in which the velocity of the vortex lattice is plotted against the current applied. From this the value of the

hitherto unmeasured velocity of the vortex lattice can be deduced, as well as the presence of a pinning effect. These are preliminary data but they are promising, in that we have large signals, and there is much rich detail which is still not interpreted. A broad range of investigations can now be undertaken on this, as well as on other systems.

Let us summarize briefly a number of applications of this technique. (i) Whenever any magnetic microstructure has a characteristic length between 100 A and 100,000 A it can be studied by these methods, with a variety of atoms used in the beam. Even if there is no great spatial regularity, we can still find out something about the magnetic field distributions. (ii) We can measure either x and y components of the oscillating field or z components if we wish to, by working with state-selected beams. While time-of-flight analysis of the velocity distribution was simple and convenient initially, we could retrieve at least a factor of 20 in signal-to-noise ratio by working with one velocity at a time with the aid of a velocity selector. (iii) We can measure the z dependence of the magnetic field by plating on a rare gas. (iv) It would be very interesting

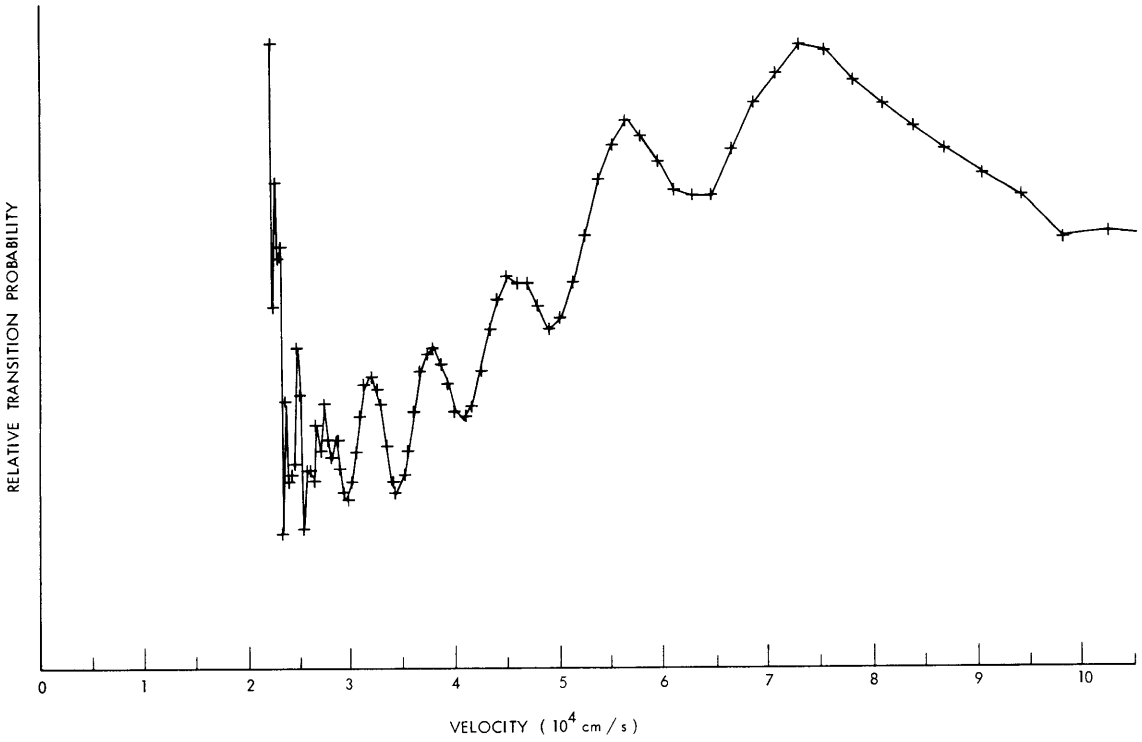

Fig. I-7. Relative transition probability normalized with respect to the maximum attainable with RF as a function of velocity. The nonsinusoidal oscillation is consistent with the Fourier components seen by an atom passing over a triangular lattice of moving vortices.

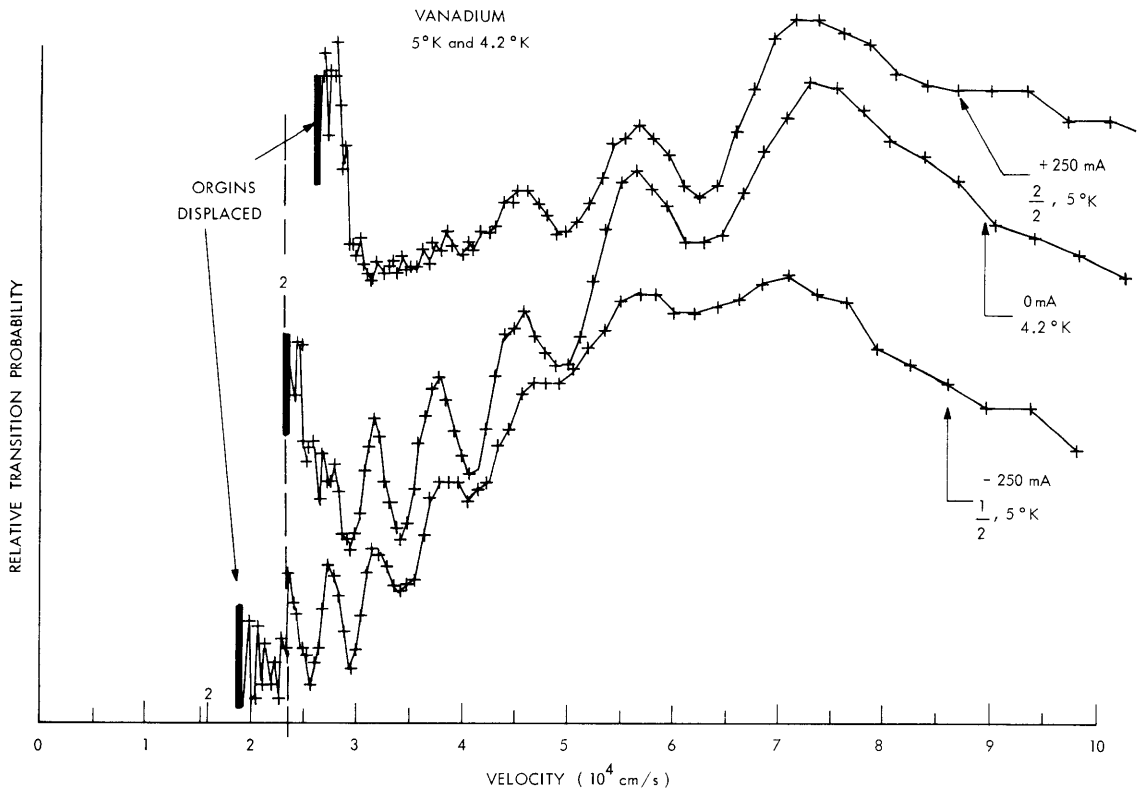

Fig. I-8. Effect of current through the sample. The middle curve with no current is the same as that of Fig. I-7, whereas the upper curve with 250 mA has been displaced toward high velocity for best fit; the lower curve with the current in the opposite direction has been displaced toward slower velocity. The washing out of different parts of these curves is not understood.

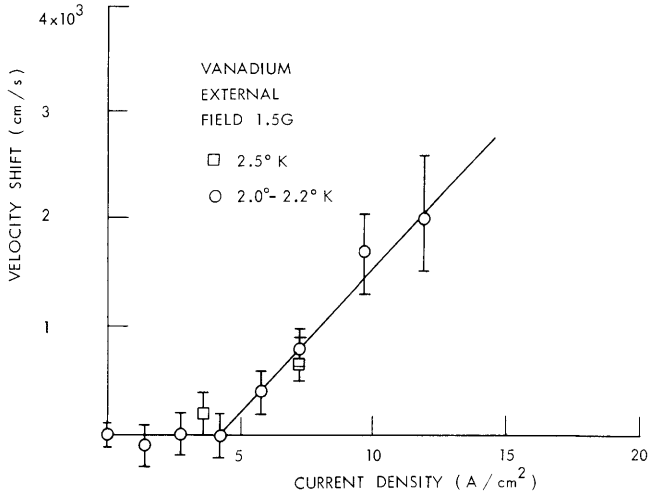

Fig. I-9.

Vortex lattice velocity as a function of current density in the sample. The inset shows the geometry of the arrangement. The effects of pinning can be seen, in that a current density of 5 A/cm^2 can flow before the vortices start moving. The slope of the curve is approximately 170 $cm^3/sec\ A$.

to study how the vortices peel off from and rejoin the diamagnetic current by studying the transitions induced by magnetic fields near the edge of the sample. This merely emphasizes (v) that we can measure small time-variant phenomena in small regions. (vi) Several other systems immediately suggest themselves, such as ferromagnetic domains, motions of domain boundaries, and phase transitions. It is also possible that magnetic variations arising from the de Haas-Van Alphen effect can be studied by this method. (vii) By using electric resonance with suitable molecules, periodic electric fields of the surfaces of a ferroelectric, for instance, could also be investigated.

During the coming year, we would like to continue refinement of the technique, the exploration of various superconducting systems, and possibly if this progresses well, the investigation of fluctuating fields associated with phase transitions in thin films of ferromagnetic materials.

T. R. Brown, J. G. King

References

1. H. Träuble and U. Essmann, J. Appl. Phys. 39, 4052 (1968).

C. CONSTRUCTION OF A SCANNING MOLECULAR MICROSCOPE

During the past year, a prototype model of a scanning molecular microscope has been designed and constructed, and is now in the preliminary testing stages. By molecular microscope we mean an instrument that "sees" by neutral molecules rather than photons, electrons, or ions. That is to say, spatial variation in the emission (usually called evaporation in the case of molecules), scattering or transmission of neutral molecules from a specimen surface is converted into a visible image. This new method for studying surfaces utilizes the weak chemical interaction which primarily determines the properties of all substances, biological and others.

The first molecular microscope is a pinhole device (see Fig. I-10) which has been designed to study specimen surfaces using neutral water molecules. Provided

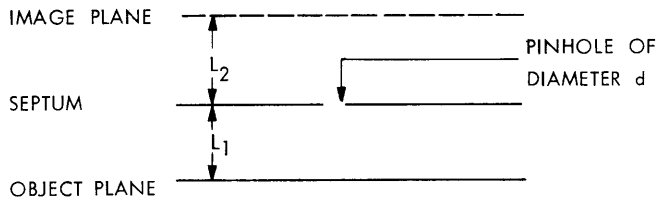

Fig. I-10. Pinhole device for studying specimen surfaces.

the mean-free path is sufficiently long, water molecules evaporating from the specimen surface are imaged by the pinhole at the image plane for any value of L_2. Initially, we shall use $L_1 = L_2 = 3 \times 10^{-1}$ cm, and these values give a minimum resolvable length (referred to the specimen) of approximately 50 μ. If we imagine the entire image to be comprised of a grid, the mesh area is a minimum resolvable area (MRA) of $\sim 2.5 \times 10^{-5}$ cm^2.

The field of view (square) contains approximately 8×10^3 MRA, which should be sufficient for a crude picture. We shall attempt to make pictures in the following way. A field ionizing detector (active area of 5×10^{-11} cm^2) which ionizes all neutral molecules incident upon it, can be scanned in both dimensions within the image plane. The resulting ions are accelerated into an electron multiplier, and generate a signal current proportional to the intensity of incident molecules at the detector at that point in the image plane. An oscilloscope is scanned synchronously by the same signal that scans the detector and is Z-modulated by the signal current. Finally, an ordinary camera on time exposure views the oscilloscope and provides the final, visual output in the form of a picture of the evaporation intensity.

The expected signal-counting rate, n_s, at the detector is obtained from kinetic theory. We have designed the first instrument to use neutral water molecules, and expect for our anticipated operating conditions a signal of

$$n_s = \frac{(3.5 \times 10^{22}) p_1 A_{MRA}}{\sqrt{M_1 T_1}} \quad \frac{A_{DET}}{\pi (L_1 + L_2)^2}$$

$$\approx 1.7 \times 10^3,$$

where

M_1 = Molecular weight of neutral molecules (water)

$= 1.8 \times 10^1$

T_1 = temperature of specimen

$= 2.1 \times 10^2$ °K

p_1 = vapor pressure of water at T_1

$= 3 \times 10^{-3}$ Torr.

The presence of residual gas (mostly N_2) in the image-plane region is also detected by our detector, and gives a background counting rate of

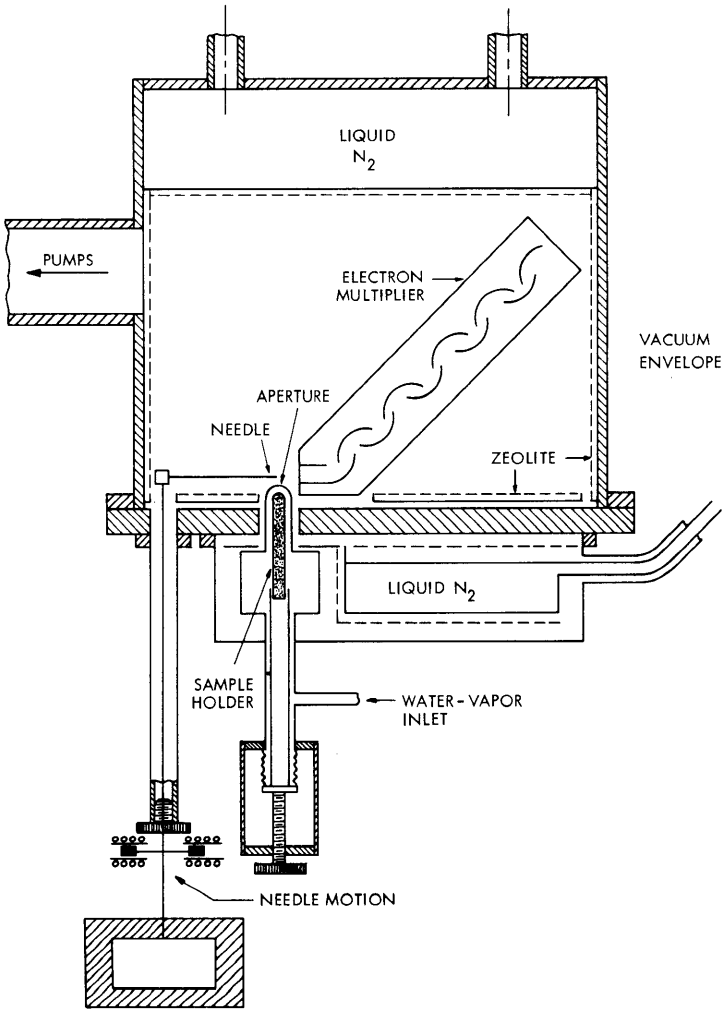

Fig. I-11. First prototype scanning molecular microscope.

$$n_B = \frac{(3.5\times10^{22})p_2 A_{DET}}{\sqrt{M_2 T_2}}$$

$$\approx (3.6\times10^{10})p_2,$$

where $M_2 = 2.8 \times 10^1$, $T_2 = 7.7 \times 10^1$ °K here.

If the scan time for a single MRA is t, then the total signal for that MRA can be taken as $N_s = n_s t$, and the noise is $\Delta N = \sqrt{(n_s+n_B)t}$. If we want K distinguishable intensity levels (shades of gray) for an MRA, we use

$$K = N_s/\Delta N = n_s\sqrt{t}/\sqrt{n_s + n_B}$$

to determine t. For K = 10 we expect $t = 7 \times 10^{-2}$ s and a total scan time of 2.4 min. These conditions should yield a crude but useful picture, and should allow demonstration of the principle of the instrument.

A sketch of our first prototype is shown in Fig. I-11. Scanning is accomplished by driving a two-dimensional magnetic-mechanical spring with an electronic scan signal, with the field-ionizing detector (needle) located at the end of a 40-cm mechanical arm. The pinhole (25 μ in diameter) is located in a 0.001" foil which is centered in a copper dome. The specimen can be mounted on a vertically adjustable stalk, with provision for temperature monitoring and heating.

Although most of the walls surrounding the detector are covered with liquid-nitrogen temperature zeolite, the background pressure (p_B) achieved thus far is not yet quite as low as expected. Nevertheless, initial picture taking with a pressure of $p_2 = 10^{-7}$ Torr clearly shows a variation in the flux of molecules onto the needle which is correlated with a source of molecules in the apparatus.

The first instrument operates in a "universal mode," detecting all neutral molecules without regard to species. Certainly, a "mass spectrometer mode" may be quite beneficial in many applications, and could be incorporated straightforwardly in future versions. Even more promising is the potential for molecular photography, by which we mean the direct conversion by chemical-physical means of molecular rays into a useful, visible image. Some initial work on molecular photography has already been done; the motivation for doing so is the realization that the ability to use all of the neutral molecules imaged by the pinhole leads to the possibility of 2000 Å resolution for 100-sec exposures with a relatively simple pinhole microscope.

J. C. Weaver, J. G. King